

Masked and Permuted Implicit Context Learning for Scene Text Recognition

Xiaomeng Yang, Zhi Qiao, Jin Wei, Dongbao Yang, Yu Zhou

Abstract—Scene Text Recognition (STR) is difficult because of the variations in text styles, shapes, and backgrounds. Though the integration of linguistic information enhances models’ performance, existing methods based on either permuted language modeling (PLM) or masked language modeling (MLM) have their pitfalls. PLM’s autoregressive decoding lacks foresight into subsequent characters, while MLM overlooks inter-character dependencies. Addressing these problems, we propose a masked and permuted implicit context learning network for STR, which unifies PLM and MLM within a single decoder, inheriting the advantages of both approaches. We utilize the training procedure of PLM, and to integrate MLM, we incorporate word length information into the decoding process and replace the undetermined characters with mask tokens. Besides, perturbation training is employed to train a more robust model against potential length prediction errors. Our empirical evaluations demonstrate the performance of our model. It not only achieves superior performance on the common benchmarks but also achieves a substantial improvement of 9.1% on the more challenging **Union14M-Benchmark**.

Index Terms—OCR, scene text recognition, language modeling, autoregressive, non-autoregressive

I. INTRODUCTION

SCENE Text Recognition (STR) [1], [2], [3], [4], [5] aims to identify characters in natural scene images, which cannot only use visual information because of the variations of scene text in style, shape, and background. Therefore, integrating linguistic knowledge into STR models has attracted extensive attention. Prior works [6], [7], [8] have achieved promising performance using external language models (LM). However, the independence between the vision model and LM may cause erroneous rectifications. Thus, an internal LM able to influence the visual space may be a better choice.

The emergence of permuted language modeling (PLM) [9] and masked language models (MLM) [10] have inspired the STR community to adopt novel decoding strategies. PARSeq [11] uses an ensemble of permuted AR decodings to train the model but the serial procedure limits the LM’s ability to anticipate future characters. As illustrated in Fig. 1(a), when recognizing the fourth character in the

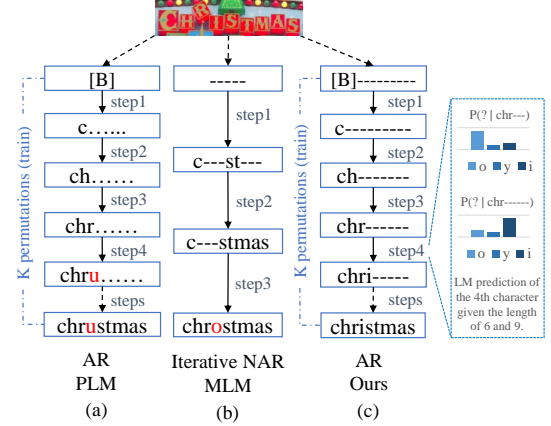


Fig. 1. Decoding procedures of PLM, MLM, and our unified language modeling. “-” in the figure represents the mask token used in decoding. The lack of global information and inadequate linguistic learning leads to misrecognition of PLM and MLM based methods.

word, the model lacks knowledge of the remaining characters, leading to the misrecognition. Conversely, MLM-based methods like PIMNet [12] offer global positional information about the entire text but may neglect dependency among each predicted character. As shown in Fig. 1(b), this approach lacks contextual knowledge among characters predicted within the same iteration, such as “m”, “a” and “s” all determined in step 2. In summary, both approaches have limitations. To improve STR performance, a more comprehensive context-learning method is needed.

Based on the above analysis, we propose a masked and permuted implicit context learning network for STR (MPSTR). Inspired by [13], we combine PLM and MLM into a single decoder by rearranging tokens. Traditional iterative MLM decoders operate through cycles of prediction followed by re-masking. However, by defining a re-masking strategy in advance, the process can mirror AR decoding behaviors, but with additional context provided by the positional information of mask tokens. In our approach, the intrinsic permutations of PLM can serve as the “re-masking strategy”, determining the decoding order. Thus, the training procedure of our model follows PLM, but in each iteration, learnable mask tokens are appended behind the recognized characters to shape the context for the succeeding iteration. Additionally, since the single PLM decoder attends solely to previous tokens during inference, randomly predicted characters following the ending symbol cannot impact its prediction. However, incorporating MLM with redundant mask tokens demands length prediction.

This work was supported by the National Natural Science Foundation of China (Grant NO 62376266), and by the Key Research Program of Frontier Sciences, CAS (Grant NO ZDBS-LY-7024). (Corresponding author: Yu Zhou.)

X. Yang, D. Yang and Y. Zhou are with the Institute of Information Engineering, Chinese Academy of Sciences, also with the School of Cyber Security, University of Chinese Academy of Sciences, Beijing 100089, China (e-mail: yangxiaomeng@iie.ac.cn; yangdongbao@iie.ac.cn; zhouyu@iie.ac.cn).

Z. Qiao is with the Tomorrow Advancing Life, Beijing 100080, China (e-mail: qiaozhi1@tal.com).

J. Wei is with the Lenovo Research, Beijing 100094, China (e-mail: weijin4@lenovo.com).

To solve this problem, we introduce an explicit length prediction using a simple learnable length token in the encoder. Specifically, the number of appended mask tokens is set to the number of un-transcribed characters in the current iteration, which enables more precise global information. For instance, the combination of the recognized “chr” and appended six mask tokens shape the context for recognizing “i” in Fig. 1(c). Besides, to address potential inaccuracies in length prediction during inference, we employ a perturbation training strategy. Our approach intends to learn an advanced internal LM by uniquely incorporating mask tokens and length information to provide global linguistic knowledge. This differs from previous methods [14], [15], [16], which directly use the length as an additional supervision.

We conduct extensive experiments to evaluate our method. Our MPSTR demonstrates superior performance on both six common benchmarks and the more challenging Union14M-Benchmark. The contributions are summarized as follows:

- We propose a STR model that leverages the unification of PLM and MLM in a single decoder, inheriting their advantages and learning superior linguistic information.
- To integrate MLM, we employ a simple yet effective length prediction method using a learnable token in the encoder, along with perturbation training, which enhances the quality of global context information.
- Noticing mislabeled images in benchmarks, we conduct verification and provide the cleansed version in github.com/Xiaomeng-Yang/STR-benchmark-cleansed to ensure a more accurate evaluation of STR models.
- Our model achieves state-of-the-art performance on standard benchmarks and outperforms previous methods by a significant margin on the Union14M-Benchmark.

II. METHOD

Our model contains a ViT-based encoder and a Masked and Permuted Decoder (MP-decoder) as shown in Fig. 2. The encoder is used for visual feature extraction and length prediction. The MP-decoder unifies MLM and PLM to decode the visual features into the final texts.

A. ViT-based Encoder and Length Prediction

The encoder is based on ViT but instead of the original *[class]* token, we introduce a learnable *[len]* token for length prediction. Given $\mathbf{z}_{input} \in \mathbb{R}^{(N+1) \times D}$, the ViT encoder outputs the final embedding $\mathbf{z} = [\mathbf{z}_0, \mathbf{z}_1, \mathbf{z}_2, \dots, \mathbf{z}_N]$. We use \mathbf{z}_0 to predict the length of the word with two fully connected layers (FC) and an argmax layer. The word length prediction is treated as a T -class classification task, where T represents the maximum possible length. Other learned tokens $[\mathbf{z}_1, \mathbf{z}_2, \dots, \mathbf{z}_N]$ are used as input vision representations for the MP-decoder.

B. Masked and Permuted Language Modeling

Let \mathcal{Z}_T represent all possible permutations of a T -length sequence. A PLM-based method maximizes:

$$\log p(\mathbf{y}|\mathbf{x}) = \mathbb{E}_{\mathbf{z} \sim \mathcal{Z}_T} \left[\sum_{t=1}^T \log p_{\theta}(y_{z_t} | \mathbf{y}_{\mathbf{z}_{<t}}, \mathbf{x}) \right] \quad (1)$$

TABLE I
THE ATTENTION MASK \mathbf{m}_{attn} FOR PERMUTATION[1, 3, 2]. 1 MEANS THE TOKEN IN THE TABLE HEADER IS MASKED WHEN DECODING.

	\underline{B}	y_1	y_2	y_3	\underline{E}	\underline{M}	\underline{M}	\underline{M}	\underline{M}	\underline{M}
y_1	0	1	1	1	1	1	0	0	0	0
y_2	0	0	1	0	1	1	1	0	1	0
y_3	0	0	1	1	1	1	1	0	0	0
\underline{E}	0	0	0	0	1	1	1	1	1	0

where z_t and $\mathbf{z}_{<t}$ denote the t -th character and the previous $t - 1$ characters in the specific permutation \mathbf{z} . For iterative MLM decoding, the model predicts all characters currently masked first and then re-masks some characters based on the predetermined strategy, such as easy-first [12]. Let \mathcal{K}_i represent masked positions in iteration i , I be the number of iterations, $\mathbf{y}_{\setminus \mathcal{K}_i}$ be determined characters and $\mathbf{M}_{\mathcal{K}_i}$ be mask tokens. An iterative MLM-based NAR decoder maximizes:

$$\log p(\mathbf{y}|\mathbf{x}) \approx \sum_{i=1}^I \sum_{k \in \mathcal{K}_i} \log p_{\theta}(y_k | \mathbf{y}_{\setminus \mathcal{K}_i}, \mathbf{M}_{\mathcal{K}_i}, \mathbf{x}) \quad (2)$$

To unify PLM and MLM, we analyze the c -th step of AR decoding in a chosen permutation of PLM, where the characters $\mathbf{y}_{\mathbf{z}_{<c}}$ are already generated. In this situation, the MLM decoder masks the characters $\mathbf{y}_{\mathbf{z}_{\geq c}}$ and will predict them depending on previously deduced tokens $\mathbf{y}_{\mathbf{z}_{<c}}$ and the subsequent mask tokens $\mathbf{M}_{\mathbf{z}_{\geq c}}$. Thus, we can unify PLM and MLM into one decoder such that when generating the next character autoregressively in each permutation, the unified MP-decoder should depend on both the predicted part and several mask tokens whose number is equal to the number of remaining undetermined characters. The unified training objective of the MP-decoder is formulated as:

$$\mathbb{E}_{\mathbf{z} \sim \mathcal{Z}_T} \left[\sum_{t=c}^T \log p_{\theta}(y_{z_t} | \mathbf{y}_{\mathbf{z}_{<t}}, \mathbf{M}_{\mathbf{z}_{\geq c}}, \mathbf{x}) \right], \quad (3)$$

C. Masked and Permuted Decoder

The MP-decoder adopts two Multi-Head Cross-Attention (MHCA) modules. The first MHCA receives position query \mathbf{p} with length $T + 1$ for an additional *[EOS]* token:

$$\mathbf{h}_c = \mathbf{p} + \text{MHCA}(\mathbf{p}, \mathbf{c}, \mathbf{c}, \mathbf{m}_{attn}, \mathbf{m}_{pad}) \quad (4)$$

where $\mathbf{c} = [\mathbf{c}_{word}; \mathbf{c}_{mask}] \in \mathbb{R}^{2(T+2) \times D}$ is the concatenation of word context embeddings $\mathbf{c}_{word} \in \mathbb{R}^{(T+2) \times D}$ and mask context embeddings $\mathbf{c}_{mask} \in \mathbb{R}^{(T+2) \times D}$, both of which are added with positional information as shown in Fig. 2. $\mathbf{m}_{attn} \in \mathbb{R}^{(T+1) \times 2(T+2)}$ and $\mathbf{m}_{pad} \in \mathbb{R}^{2(T+2)}$ are the attention mask and padding mask, respectively. Since we cannot train on all $L!$ permutations, we choose K permutations from \mathcal{Z}_L , and the chosen permutations are informed to the decoder through the attention mask. The attention mask $\mathbf{m}_{attn} = [\mathbf{m}_{wattn}; \mathbf{m}_{mattn}]$ is generated uniquely for each chosen permutation according to equation (3), where \mathbf{m}_{wattn} and \mathbf{m}_{mattn} are attention masks for \mathbf{c}_{word} and \mathbf{c}_{mask} , respectively. At a certain step of AR decoding, the unpredicted part of the word context embeddings and the mask context embeddings corresponding to the predicted tokens are masked,

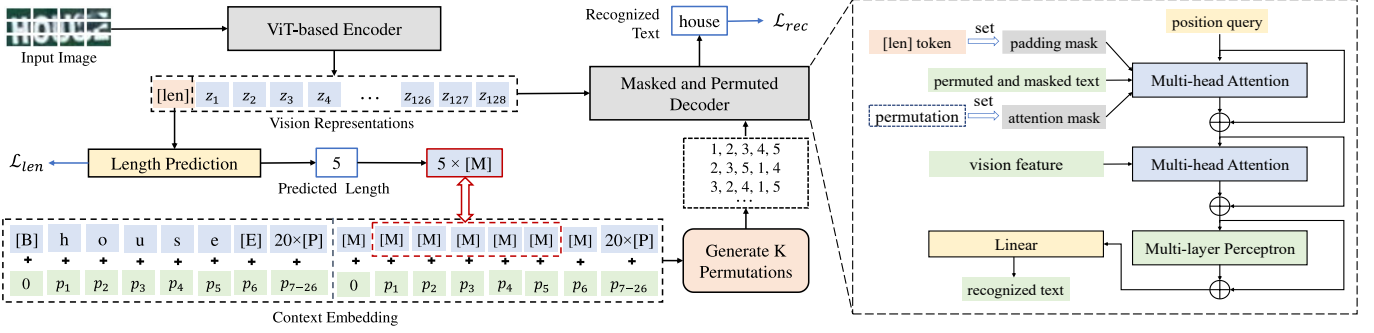


Fig. 2. Architecture of the proposed method. [B], [E], [P] and [M] stands for the beginning-of-sequence, end-of-sequence, padding and mask tokens, respectively. The ViT-based encoder provides the text length using the [len] token. Then, the predicted length number of mask tokens is appended. After K permutation operations, the masked and permuted text is input to the decoder for the corresponding prediction.

e.g. the example in Table I. When decoding the character y_3 , [B] and y_1 in c_{word} , and the last three [M] in c_{mask} could be attended. The padding mask is determined by the predicted word length L with the first $L + 2$ tokens unmasked for both c_{word} and c_{mask} . In other words, $\mathbf{m}_{pad} = [\mathbf{m}_{wpad}; \mathbf{m}_{mpad}]$, where $\mathbf{m}_{wpad} = \mathbf{m}_{mpad}$. For the word “house” with length 5, $\mathbf{m}_{wpad} = \mathbf{m}_{mpad} = [1, 1, 1, 1, 1, 1, 0, \dots, 0] \in \mathbb{R}^{T+2}$. The second MHCA computes the attention between \mathbf{h}_c and image visual features \mathbf{z}_v obtained from the ViT encoder. After that, the prediction is ultimately achieved by processing the output logits through an MLP and an FC layer.

D. Training Objective and Strategies

The objective function of our proposed method is:

$$\mathcal{L} = \lambda \mathcal{L}_{len} + (1 - \lambda) \mathcal{L}_{rec} \quad (5)$$

where \mathcal{L}_{len} represents the loss of length prediction, and \mathcal{L}_{rec} stands for the recognition loss. The parameter λ is employed to balance the two losses. We use the cross-entropy loss for \mathcal{L}_{len} . For recognition loss, we compute the mean of the cross-entropy losses for K chosen permuted decoding orders. During training, we employ a teacher-forcing strategy, using the ground truth length to set the masks. For inference, we use the predicted length. Additionally, to enhance the robustness of the decoder against the potential length prediction errors during inference, we adopt a perturbation training strategy. For each batch, we perturb the ground truth length for a randomly selected subset of images, either by adding or subtracting one.

III. EXPERIMENTS

A. Datasets

We use three groups for training: (1) Synthetic data (S): MJSynth [23] and SynthText [24], (2) Real images [11] (R), and (3) Union14M-L’s training set [22]. For evaluation, we assess the models on six benchmarks: IIIT5k-word (IIIT5k) [25], ICDAR 2013 (IC13) [26], Street View Text (SVT) [27], ICDAR 2015 (IC15) [28], SVT-Perspective (SVTP) [29], and CUTE80 (CUTE) [30]. However, there are some mislabeled images, so we perform further verification based on [3]. Additional details can be found in our supplementary file. We also test our models on the Union14M-Benchmark [22].

B. Implementation Details

We employ the small and base DeiT [35] for MPSTR and MPSTR-B with 128×32 images and 8×4 patches. Our model uses 36-char for common benchmarks and 91-char for Union14M. Data augmentations are consistent with PARSeq [11]. We employ the Adam optimizer with the 1cycle [36] scheduler for the initial 85% iterations and the Stochastic Weight Averaging scheduler for others. Parameters are set to $T = 25$, $K = 12$ and $\lambda = 0.25$. The models are trained for 254,520 iterations on S and R, and 10 epochs on Union14M-L on NVIDIA Tesla V100. One Refinement is used employing the cloze mask for AR and two for NAR like [11]. Word accuracy is assessed ignoring cases and symbols.

C. Comparison with State-of-the-Art

1) *Union14M-Benchmark*: We highlight our method’s performance on the Union14M-Benchmark. As detailed in Table II, our models surpass the previous best approach by an average of 9.1%. Notably, on the multi-oriented dataset, our model exceeds the previous best by 19.2%, attributable to our robust linguistic modeling. Besides, while our approach lags behind language-free methods on incomplete images due to semantic dependencies, the word length prediction mitigates this impact, so it is better than other language-based methods.

2) *Common Benchmarks*: We evaluate models on cleansed benchmarks with reproduction for PARSeq [11] using its official configuration and PIMNet [12] using the DeiT-small encoder. As shown in Table III, our approach achieves comparable results when trained on both S and R. It surpasses LevOCR [34] by 0.2%, but with only a third of inference time. Compared with the PLM-based PARSeq, our AR model improves accuracy over PARSeq_A by 0.6% and 0.3%, and our NAR model beats PARSeq_N with boosts of 0.7% and 0.9%. MPSTR_N even matches the performance of PARSeq_A with a latency reduction of about 5ms. In comparison with MLM-based methods, MPSTR_N betters PIMNet by 1.0% and 1.5%.

D. Ablation Study

1) *Language Modeling Method*: As shown in Table IV, the baseline left-to-right AR model makes NAR inference

TABLE II
RECOGNITION RESULTS ON UNION14M-BENCHMARK. “N” AND “A” REPRESENT NAR AND AR DECODINGS, RESPECTIVELY.

Method	Curve	Multi-Oriented	Artistic	Contextless	Salient	Multi-Words	General	Avg	Incomplete (\downarrow)
CRNN [17]	19.4	4.5	34.2	44.0	16.7	35.7	60.4	30.7	0.9
SAR [18]	68.9	56.9	60.6	73.3	60.1	74.6	76.0	67.2	2.1
SATRN [19]	74.8	64.7	67.1	76.1	72.2	74.1	75.8	72.1	0.9
SRN [6]	49.7	20.0	50.7	61.0	43.9	51.5	62.7	48.5	2.2
ABINet [7]	75.0	61.5	65.3	71.1	72.9	59.1	79.4	69.2	2.6
VisionLAN [20]	70.7	57.2	56.7	63.8	67.6	47.3	74.2	62.5	<u>1.3</u>
SVTR [21]	72.4	68.2	54.1	68.0	71.4	67.7	77.0	68.4	2.0
MATRN [8]	80.5	64.7	71.1	74.8	79.4	67.6	77.9	74.6	1.7
MAERec-S [22]	75.4	66.5	66.0	76.1	72.6	77.0	80.8	73.5	3.5
MAERec-B [22]	76.5	67.5	65.7	75.5	74.6	<u>77.7</u>	81.8	74.2	3.2
MPSTR _N (Ours)	82.4	80.9	70.6	77.0	79.1	71.5	81.4	77.6	1.4
MPSTR _A (Ours)	84.0	83.1	71.8	78.3	80.1	76.7	82.4	79.5	<u>1.3</u>
MPSTR-B _N (Ours)	85.9	85.0	74.6	80.4	81.7	75.2	83.2	80.9	1.5
MPSTR-B _A (Ours)	87.8	87.4	77.2	83.1	83.6	82.2	84.3	83.7	1.5

TABLE III
RECOGNITION RESULTS ON CLEANSSED SIX BENCHMARKS. * INDICATES THAT THE REPRODUCED MODELS. MGP-STR[†] REPRESENTS THE SMALL CONFIGURATION. S¹ LM PRETRAINED ON WIKITEXT-103 [31].

Method	Train Data	IIIT5K	IC13	SVT	IC15	SVTP	CUTE	Avg	Time (ms/img)
TRBA [3]	S	90.5	93.3	87.3	79.0	78.5	72.9	85.9	16.7
ViTSTR [32]	S	88.9	92.6	87.2	80.5	82.3	80.9	86.2	7.92
SRN [6]	S	92.2	95.2	89.6	81.7	85.1	88.5	88.9	12.1
VisionLAN [20]	S	96.5	96.3	90.4	85.4	85.7	88.9	91.9	14.8
PIMNet* [12]	S	95.5	95.9	92.0	86.5	87.9	90.6	92.1	15.6
ABINet [7]	S ¹	97.0	97.0	93.4	87.3	89.6	89.2	93.3	23.4
MGP-STR [†] [33]	S	95.6	96.6	93.0	87.8	89.0	88.5	92.7	9.37
PARSeq _N * [11]	S	96.0	96.6	92.4	86.8	88.7	90.6	92.6	11.7
PARSeq _A * [11]	S	96.6	97.0	92.7	87.8	89.3	91.7	93.3	17.5
LevOCR [34]	S	<u>97.1</u>	96.7	94.4	<u>88.4</u>	89.6	<u>90.6</u>	<u>93.7</u>	60.5
MPSTR _N (Ours)	S	96.8	96.4	92.6	88.2	88.5	91.7	93.3	12.6
MPSTR _A (Ours)	S	97.2	96.9	<u>93.2</u>	89.0	89.6	91.7	93.9	19.1
PIMNet* [12]	R	97.7	97.1	96.5	90.9	92.9	95.1	95.3	15.6
PARSeq _N [11]	R	98.1	97.9	97.2	92.8	94.0	98.6	96.3	11.7
PARSeq _A [11]	R	98.9	<u>98.3</u>	97.5	<u>93.7</u>	<u>95.7</u>	98.6	97.1	17.5
MPSTR _N (Ours)	R	<u>99.0</u>	98.4	<u>98.3</u>	<u>93.7</u>	95.5	<u>98.6</u>	<u>97.2</u>	12.6
MPSTR _A (Ours)	R	99.2	<u>98.3</u>	98.5	93.9	96.1	99.0	97.4	19.1

TABLE IV
ABLATION STUDY ON LANGUAGE MODELING STRATEGY. BASELINE IS AN AR MODEL. * MODEL EVALUATED WITH THE GT LENGTHS. (R/S) INDICATES THE TRAINING DATA.

Method	AR (R)	NAR (R)	AR (S)	NAR (S)
baseline	96.63	0.00	93.12	0.00
PLM	97.10	96.33	93.25	92.58
PLM+MLM	97.43	97.21	93.86	93.29
PLM+MLM*	97.71	97.67	94.44	94.18

inapplicable. Incorporating PLM facilitates NAR decoding by learning linguistic relationships. MLM further enhances both AR and NAR accuracy thanks to its global contextual insights. An upper bound is given in the final row. Our integrated language modeling has superior context comprehension, driven by global context and comprehensive character dependencies.

2) *MLM Integration*: Table V reveals that merely introducing mask tokens without length supervision prohibits NAR inference. This is expected, as our unified likelihood defined in equation (3) necessitates the number of unpredicted tokens. Solely adding the predicted length embedding to the first MHCA’s query also cannot provide satisfying results because of imprecise length predictions. It suggests that both mask tokens and length are required to incorporate MLM.

TABLE V
ABLATION STUDY OF MLM INTEGRATION.

Mask Token	Length	AR (R)	NAR (R)	AR (S)	NAR (S)
\times	\times	97.10	96.33	93.25	92.58
\checkmark	\times	96.83	53.42	93.36	36.58
\times	\checkmark	96.67	96.39	93.23	92.54
\checkmark	\checkmark	97.43	97.21	93.86	93.29

TABLE VI
ABLATION STUDY ABOUT LENGTH PREDICTION METHODS.

Method	Real Data		Synthetic Data		Length	
	AR	NAR	AR	NAR	Real	Synth
Char	96.74	96.04	92.80	91.63	98.44	95.41
Word	97.43	97.21	93.86	93.29	98.79	96.41

TABLE VII
MPSTR_N’S RECONIGNTION RESULTS VS PERTURBATION RATIO.

Data	0%	25%	33%	50%	66%	75%
S	92.09	92.47	92.55	92.74	93.10	92.80
R	96.72	96.81	97.21	96.73	-	-

3) *Word Length Prediction*: Two methods of length prediction are available: character-level prediction, which determines the presence of each character, and word-level prediction, which directly estimates the word’s length. We use a parallel decoder for binary classification at each position for character-level prediction, and the length token for word-level prediction. As shown in Table VI, the word-level approach performs better since it utilizes global information.

4) *Perturbation training*: Table XI reveals that models trained on S need a higher proportion of perturbed images (66%) due to their regularity, while models trained on R perform best with just 33% perturbed images.

IV. CONCLUSION

We propose MPSTR to overcome the limitations of PLM and MLM, learning a more effective internal LM with advanced linguistic information. Additionally, word-level text length prediction with perturbation training is introduced to effectively integrate the MLM method. Our method achieves SOTA performance on most public benchmarks and shows consistent improvements on the challenging Union14M-Benchmark, validating its effectiveness.

REFERENCES

- [1] Y. Zhu, C. Yao, and X. Bai, "Scene text detection and recognition: Recent advances and future trends," *Frontiers of Computer Science*, vol. 10, no. 1, pp. 19–36, 2016.
- [2] B. Shi, M. Yang, X. Wang, P. Lyu, C. Yao, and X. Bai, "Aster: An attentional scene text recognizer with flexible rectification," *IEEE transactions on pattern analysis and machine intelligence*, vol. 41, no. 9, pp. 2035–2048, 2018.
- [3] J. Baek, G. Kim, J. Lee, S. Park, D. Han, S. Yun, S. J. Oh, and H. Lee, "What is wrong with scene text recognition model comparisons? dataset and model analysis," in *Proceedings of the IEEE/CVF international conference on computer vision*, 2019, pp. 4715–4723.
- [4] Z. Qiao, Y. Zhou, D. Yang, Y. Zhou, and W. Wang, "Seed: Semantics enhanced encoder-decoder framework for scene text recognition," in *Proceedings of the IEEE/CVF Conference on Computer Vision and Pattern Recognition*, 2020, pp. 13 528–13 537.
- [5] S. Long, X. He, and C. Yao, "Scene text detection and recognition: The deep learning era," *International Journal of Computer Vision*, vol. 129, no. 1, pp. 161–184, 2021.
- [6] D. Yu, X. Li, C. Zhang, T. Liu, J. Han, J. Liu, and E. Ding, "Towards accurate scene text recognition with semantic reasoning networks," in *Proceedings of the IEEE/CVF Conference on Computer Vision and Pattern Recognition*, 2020, pp. 12 113–12 122.
- [7] S. Fang, H. Xie, Y. Wang, Z. Mao, and Y. Zhang, "Read like humans: Autonomous, bidirectional and iterative language modeling for scene text recognition," in *Proceedings of the IEEE/CVF Conference on Computer Vision and Pattern Recognition*, 2021, pp. 7098–7107.
- [8] B. Na, Y. Kim, and S. Park, "Multi-modal text recognition networks: Interactive enhancements between visual and semantic features," in *European Conference on Computer Vision*. Springer, 2022, pp. 446–463.
- [9] Z. Yang, Z. Dai, Y. Yang, J. Carbonell, R. R. Salakhutdinov, and Q. V. Le, "Xlnet: Generalized autoregressive pretraining for language understanding," *Advances in neural information processing systems*, vol. 32, 2019.
- [10] J. Devlin, M.-W. Chang, K. Lee, and K. Toutanova, "Bert: Pre-training of deep bidirectional transformers for language understanding," *arXiv preprint arXiv:1810.04805*, 2018.
- [11] D. Bautista and R. Atienza, "Scene text recognition with permuted autoregressive sequence models," in *European Conference on Computer Vision*. Springer, 2022, pp. 178–196.
- [12] Z. Qiao, Y. Zhou, J. Wei, W. Wang, Y. Zhang, N. Jiang, H. Wang, and W. Wang, "Pimnet: a parallel, iterative and mimicking network for scene text recognition," in *Proceedings of the 29th ACM International Conference on Multimedia*, 2021, pp. 2046–2055.
- [13] K. Song, X. Tan, T. Qin, J. Lu, and T.-Y. Liu, "Mpnnet: Masked and permuted pre-training for language understanding," *Advances in Neural Information Processing Systems*, vol. 33, pp. 16 857–16 867, 2020.
- [14] Z. Xie, Y. Huang, Y. Zhu, L. Jin, Y. Liu, and L. Xie, "Aggregation cross-entropy for sequence recognition," in *Proceedings of the IEEE/CVF conference on computer vision and pattern recognition*, 2019, pp. 6538–6547.
- [15] H. Jiang, Y. Xu, Z. Cheng, S. Pu, Y. Niu, W. Ren, F. Wu, and W. Tan, "Reciprocal feature learning via explicit and implicit tasks in scene text recognition," in *Document Analysis and Recognition-ICDAR 2021: 16th International Conference, Lausanne, Switzerland, September 5–10, 2021, Proceedings, Part I*. Springer, 2021, pp. 287–303.
- [16] B. Li, Y. Yuan, D. Liang, X. Liu, Z. Ji, J. Bai, W. Liu, and X. Bai, "When counting meets hmer: Counting-aware network for handwritten mathematical expression recognition," in *Computer Vision-ECCV 2022: 17th European Conference, Tel Aviv, Israel, October 23–27, 2022, Proceedings, Part XXVIII*. Springer, 2022, pp. 197–214.
- [17] B. Shi, X. Bai, and C. Yao, "An end-to-end trainable neural network for image-based sequence recognition and its application to scene text recognition," *IEEE transactions on pattern analysis and machine intelligence*, vol. 39, no. 11, pp. 2298–2304, 2016.
- [18] H. Li, P. Wang, C. Shen, and G. Zhang, "Show, attend and read: A simple and strong baseline for irregular text recognition," in *Proceedings of the AAAI conference on artificial intelligence*, 2019, pp. 8610–8617.
- [19] T. Wang, Y. Zhu, L. Jin, C. Luo, X. Chen, Y. Wu, Q. Wang, and M. Cai, "Decoupled attention network for text recognition," in *Proceedings of the AAAI conference on artificial intelligence*, vol. 34, no. 07, 2020, pp. 12 216–12 224.
- [20] Y. Wang, H. Xie, S. Fang, J. Wang, S. Zhu, and Y. Zhang, "From two to one: A new scene text recognizer with visual language modeling network," in *Proceedings of the IEEE/CVF International Conference on Computer Vision*, 2021, pp. 14 194–14 203.
- [21] Y. Du, Z. Chen, C. Jia, X. Yin, T. Zheng, C. Li, Y. Du, and Y.-G. Jiang, "Svtr: Scene text recognition with a single visual model," in *Proceedings of the 31st International Joint Conference on Artificial Intelligence*, 2022, pp. 884–890.
- [22] Q. Jiang, J. Wang, D. Peng, C. Liu, and L. Jin, "Revisiting scene text recognition: A data perspective," *arXiv preprint arXiv:2307.08723*, 2023.
- [23] M. Jaderberg, K. Simonyan, A. Vedaldi, and A. Zisserman, "Reading text in the wild with convolutional neural networks," *International journal of computer vision*, vol. 116, no. 1, pp. 1–20, 2016.
- [24] A. Gupta, A. Vedaldi, and A. Zisserman, "Synthetic data for text localisation in natural images," in *Proceedings of the IEEE conference on computer vision and pattern recognition*, 2016, pp. 2315–2324.
- [25] A. Mishra, K. Alahari, and C. Jawahar, "Scene text recognition using higher order language priors," in *BMVC-British machine vision conference*. BMVA, 2012.
- [26] D. Karatzas, F. Shafait, S. Uchida, M. Iwamura, L. G. i Bigorda, S. R. Mestre, J. Mas, D. F. Mota, J. A. Almazan, and L. P. De Las Heras, "Icdar 2013 robust reading competition," in *2013 12th international conference on document analysis and recognition*. IEEE, 2013, pp. 1484–1493.
- [27] K. Wang, B. Babenko, and S. Belongie, "End-to-end scene text recognition," in *2011 International conference on computer vision*. IEEE, 2011, pp. 1457–1464.
- [28] D. Karatzas, L. Gomez-Bigorda, A. Nicolaou, S. Ghosh, A. Bagdanov, M. Iwamura, J. Matas, L. Neumann, V. R. Chandrasekhar, S. Lu *et al.*, "Icdar 2015 competition on robust reading," in *2015 13th international conference on document analysis and recognition (ICDAR)*. IEEE, 2015, pp. 1156–1160.
- [29] T. Q. Phan, P. Shivakumara, S. Tian, and C. L. Tan, "Recognizing text with perspective distortion in natural scenes," in *Proceedings of the IEEE International Conference on Computer Vision*, 2013, pp. 569–576.
- [30] A. Risnumawan, P. Shivakumara, C. S. Chan, and C. L. Tan, "A robust arbitrary text detection system for natural scene images," *Expert Systems with Applications*, vol. 41, no. 18, pp. 8027–8048, 2014.
- [31] S. Merity, C. Xiong, J. Bradbury, and R. Socher, "Pointer sentinel mixture models," in *International Conference on Learning Representations*, 2017. [Online]. Available: <https://openreview.net/forum?id=Byj72udxe>
- [32] R. Atienza, "Vision transformer for fast and efficient scene text recognition," in *International Conference on Document Analysis and Recognition*. Springer, 2021, pp. 319–334.
- [33] P. Wang, C. Da, and C. Yao, "Multi-granularity prediction for scene text recognition," in *European Conference on Computer Vision*. Springer, 2022, pp. 339–355.
- [34] C. Da, P. Wang, and C. Yao, "Levenshtein ocr," in *European Conference on Computer Vision*. Springer, 2022, pp. 322–338.
- [35] H. Touvron, M. Cord, M. Douze, F. Massa, A. Sablayrolles, and H. Jégou, "Training data-efficient image transformers & distillation through attention," in *International Conference on Machine Learning*. PMLR, 2021, pp. 10 347–10 357.
- [36] L. N. Smith and N. Topin, "Super-convergence: Very fast training of neural networks using large learning rates," in *Artificial intelligence and machine learning for multi-domain operations applications*, vol. 11006. SPIE, 2019, pp. 369–386.

TABLE VIII
THE AR DECODING ATTENTION MASK. 1 MEANS MASKED.

	$[B]$	y_1	y_2	...	y_L	$[E]$	$[M]_0$	$[M]_1$	$[M]_2$...	$[M]_L$	$[M]_{L+1}$
y_1	0	1	1	1	1	1	1	0	0	0	0	0
y_2	0	0	1	1	1	1	1	1	0	0	0	0
...	0	0	0	1	1	1	1	1	1	0	0	0
y_L	0	0	0	0	1	1	1	1	1	1	0	0
$[E]$	0	0	0	0	0	1	1	1	1	1	1	0

TABLE IX
THE CLOZE ATTENTION MASK FOR REFINEMENT.

	$[B]$	y_1	y_2	...	y_L	$[E]$	$[M]_0$	$[M]_1$	$[M]_2$...	$[M]_L$	$[M]_{L+1}$
y_1	0	1	0	0	0	0	1	0	1	1	1	1
y_2	0	0	1	0	0	0	1	1	0	1	1	1
...	0	0	0	1	0	0	1	1	1	0	1	1
y_L	0	0	0	0	1	0	1	1	1	1	0	1
$[E]$	0	0	0	0	0	1	1	1	1	1	1	0

APPENDIX

A. Model Evaluation

We utilize AR decoding with one refinement iteration and NAR decoding with two refinement iterations. The refinement is performed using the cloze mask.

The NAR decoding generates all tokens simultaneously with all position queries $\mathbf{p} = [\mathbf{p}_1, \mathbf{p}_2, \dots, \mathbf{p}_{T+1}]$, where T is the maximum length, and $\mathbf{p}_T + 1$ is added for the end-of sequence (eos) token. For NAR inference, we provide the beginning token $[B]$ along with $L + 2$ mask tokens $[M]$, where $[M]_0$ and $[M]_{L+1}$ represent the corresponding mask tokens for beginning token and eos token, as context.

The AR decoding generates one new token per iteration from left to right. The attention mask for the AR decoding procedure is shown in Table VIII. For the first iteration, it predicts the first token y_1 with the position query \mathbf{p}_1 , using the context set to $[B]$ concatenated with $L + 1$ mask tokens. For the succeeding iteration i , the context is set to the determined tokens (i.e. $[B]$ together with the determined characters y_1 to y_{i-1}) concatenated with the mask tokens for the unpredicted part (i.e. $[M]_i$ to $[M]_{L+1}$). We use \mathbf{p}_i as the position query.

Before each refinement, the length is re-determined based on the predicted text from the previous iteration. When decoding a character y_i , the query \mathbf{p}_i can attend to all information from the previous iteration except itself. Therefore, determined tokens and one mask token for itself are set as the context, as illustrated in Table IX. All tokens are refined simultaneously.

B. Benchmark Cleansing Details

Despite the widespread use of these existing benchmarks in scene text recognition, we have noticed that there are mislabeled images in the benchmark, as illustrated by the examples in Fig. 3. State-of-the-art STR models have achieved an accuracy over 95%. However, the common benchmarks still contain noise, and future work might continue to evaluate models on these noisy benchmarks. We consider this a serious issue, and it is why we embarked on the task of cleaning the benchmark datasets. We conduct further verification of these labels. For example, when examining the image “OPEII”, we identified the final two “II” characters as a single entity “N”

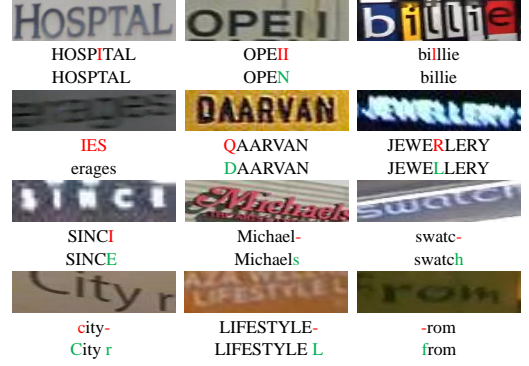


Fig. 3. Examples of label noise in benchmark datasets are presented. Characters that are mislabeled or missing are highlighted in red (top), while the corrected labels are provided below.

TABLE X
RECOGNITION ACCURACY OF MPSTR TRAINED USING REAL DATASETS ON THE BENCHMARK VS THE NUMBER OF PERMUTATIONS USED (K) FOR TRAINING. NO PERTURBATION IS APPLIED FOR THESE MODELS. AR ACC. AND NAR ACC. ARE EVALUATED WITHOUT REFINEMENT. FOR CLOZE ACC., WE USE GT LABEL AS THE INITIAL PREDICTION.

K	AR acc.	NAR acc.	cloze acc.
1	96.18	0.00	63.23
2	96.58	1.32	97.54
6	96.23	96.10	98.00
12	96.65	96.32	98.08
18	96.45	96.34	97.97

TABLE XI
MPSTR_A'S RECOGNITION RESULTS ON THE BENCHMARK VS LOSS BALANCE HYPER-PARAMETER λ WITHOUT PERTURBATION TRAINING.

λ	0.15	0.20	0.25	0.33	0.50
Acc	96.53	96.60	96.72	96.47	96.34

based on the character pitch. Even if we were to consider the last two characters as two “I”s, the shape does not match that of a capital “I”. And for “SINCI”, the shape of the last character is not like the second clear “I”. The cleansed benchmark datasets are provided to ensure a more accurate evaluation of scene text recognition models.

C. More Ablation Study Analysis

1) *Permutation Number*: Results presented in Table X highlight that the NAR decoding procedure encounters difficulties with a limited number of permutations ($K = 1, 2$). This is because there is insufficient contextual information. In contrast, AR decoding shows robust performance, primarily due to the alignment between training and inference, augmented by the length supervision. As K grows, there is a noticeable improvement in both AR and NAR performances up to $K \leq 12$. It is worth noting that our MPSTR demands more permutations for optimal performance than the PLM-based PARseq. This is attributed to the enriched global linguistic information derived from the padding of mask tokens.

2) *Balance Weight λ* : The hyper-parameter λ serves as a balancing factor between the length prediction loss L_{len} and the recognition loss L_{rec} . We conduct an ablation study on λ and present the results in Table X.